

1990

# Dynamics of Compliance Mechanisms Scroll Compressors, Part II: Radial Compliance

J. J. Nieter

*United Technologies Research Center*

Follow this and additional works at: <https://docs.lib.purdue.edu/icec>

---

Nieter, J. J., "Dynamics of Compliance Mechanisms Scroll Compressors, Part II: Radial Compliance" (1990). *International Compressor Engineering Conference*. Paper 720.

<https://docs.lib.purdue.edu/icec/720>

This document has been made available through Purdue e-Pubs, a service of the Purdue University Libraries. Please contact [epubs@purdue.edu](mailto:epubs@purdue.edu) for additional information.

Complete proceedings may be acquired in print and on CD-ROM directly from the Ray W. Herrick Laboratories at <https://engineering.purdue.edu/Herrick/Events/orderlit.html>

**DYNAMICS OF COMPLIANCE MECHANISMS IN SCROLL COMPRESSORS  
PART II: RADIAL COMPLIANCE**

Jeff J. Nieter  
Research Engineer  
United Technologies Research Center  
East Hartford, CT 06108

**ABSTRACT**

In this paper two radial compliance mechanisms are discussed for the scroll compressor: the eccentric bushing and the slider block. These two mechanisms couple the orbiting scroll hub with the crank shaft offset. Several references have discussed the eccentric bushing mechanism briefly in the past, while none have specifically discussed the slider block. This paper will discuss modeling these two approaches in more detail, and further, will discuss the dynamic characteristics of these mechanisms and their effect on scroll compressor performance over a range of different geometries.

**NOMENCLATURE**

a	Acceleration
b	Eccentricity of eccentric bushing, or slider block offset
d	Distance along slide block from shaft axis to reaction force
e	Eccentricity of orbit for orbiting scroll relative to fixed scroll
F	Force
m	Mass
r	Crank offset in eccentric bushing mechanism, or position vector
T	Torque
w	Width of slider block
$\beta$	Included angle at axis f in eccentric bushing mechanism
$\psi$	Phase angle
$\phi$	Eccentric bushing tangent angle
$\mu$	Friction coefficient
$\gamma$	Slider block offset angle
$\gamma_c$	Included angle at axis c in eccentric bushing mechanism
$\gamma_m$	Included angle at axis m in eccentric bushing mechanism
$\omega$	Angular speed of crankshaft
$\theta$	Crank angle

**Subscripts**

a	Axial component
bl	Slider block
cr	Crank offset
ec	Eccentric bushing
i	Inertia force
o	Reference value
p	Pressure force
r	Radial component
s	Seal force
sb	Scroll bearing hub
t	Tangential component

**Superscripts**

- First derivative with respect to time
- .. Second derivative with respect to time

**INTRODUCTION**

Scroll compressors are quickly gaining popularity in many applications due to their high efficiency, fewer parts, and low noise and vibration as compared to competing compressor types. It is also widely recognized that in order to achieve

high efficiency with a scroll compressor, some form of compliance mechanism is required. Radial compliance is an approach utilized in many scroll compressors; usually in the form of either an eccentric bushing (also referred to as a swing link) or a slider block type mechanism which couples the orbiting scroll hub with the crank shaft offset. Compliance in the radial direction can insure that the radial clearances at the flanks of the mating scroll wraps are minimized or eliminated, thus minimizing leakage across this sealing surface. The actuation of the orbiting scroll against the fixed scroll to close these radial flank clearances is shown in Fig. 1. Radial compliance also provides relief of high pressure during liquid ingestion, accommodates wear of material at the flanks of the fixed and orbiting scroll wraps, and reduces the effect of some manufacturing tolerances. Further, it can produce a positive sealing force at the flanks of the mating wraps, allowing some load to be supported by the wraps instead of it mostly being supported by the hub bearing. Several references[1-3] have discussed the eccentric bushing type radial compliance mechanism briefly in the past, while none have discussed the slider block to any extent.

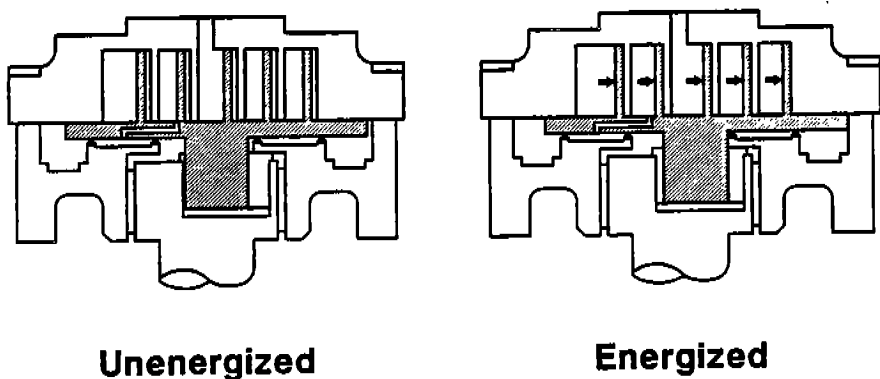


Figure 1 Actuation of radial compliance mechanism to minimize flank clearance

#### ANALYTICAL MODELING

##### Geometry

The eccentric bushing type radial compliance mechanism is shown schematically in Figs. 2a and b. In Fig. 2a, the eccentric bushing configuration utilizes a male orbiter bearing hub. The male hub fits into the journal in the eccentric bushing, and the eccentric bushing fits into a journal in the crankshaft such that the center of this journal is offset to affect the crank motion. In Fig. 2b, the eccentric bushing configuration utilizes a female orbiter hub and journal bearing into which the eccentric bushing fits. In this case, the eccentric bushing has a journal in it to accept the crank post which affects the crank motion. Radial compliance is accomplished in both of these configurations by allowing the eccentric bushing to rotate relative to the crankshaft. Consequently the orbiter can move in or out radially relative to the crankshaft and fixed scroll. A kinematic model for both of these configurations is shown in Fig. 3. The origin of the  $x$  and  $y$  axes is labeled  $f$  to indicate the axis of the fixed scroll and crankshaft. The point labeled  $m$  indicates the axis of the moving or orbiting scroll, while the point labeled  $c$  indicates the axis of the crank offset or throw. The crank offset is represented by  $r$ , while  $e$  is the eccentricity of orbit,  $b$  is the eccentricity of the bushing, and  $\theta$  is the crank angle. Also labeled in Fig. 3 are the tangent and radial lines to the orbiting scroll at  $m$ . Between the tangent line at  $m$  and the line passing through points  $c$  and  $m$  is the angle referred to as the tangent angle of the eccentric bushing. The performance of an eccentric bushing radial compliance mechanism will be shown to be significantly effected by the tangent angle and the crank offset.

The other type of radial compliance mechanism considered here is the slider block which is shown schematically in Fig. 4. In this mechanism, the radial compliance is achieved simply by allowing the block to slide out so that the orbiting scroll can maintain contact at the wrap flanks with the fixed scroll. A

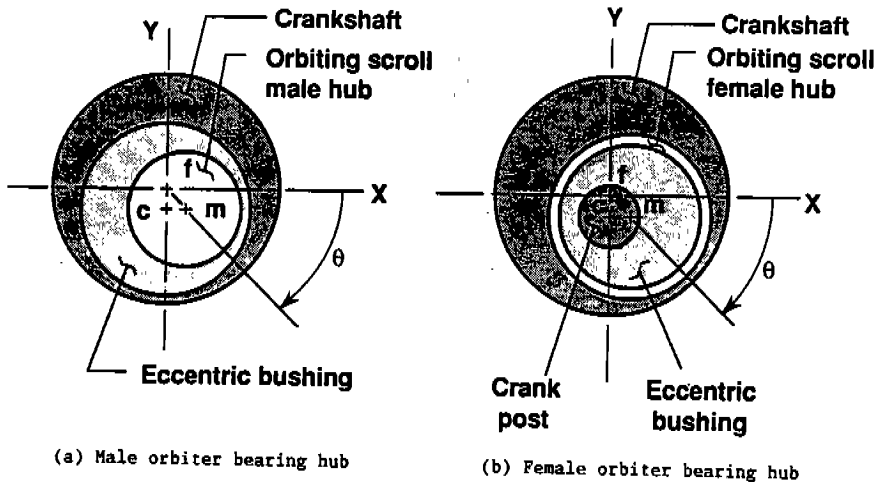


Figure 2 Eccentric bushing type radial compliance mechanism

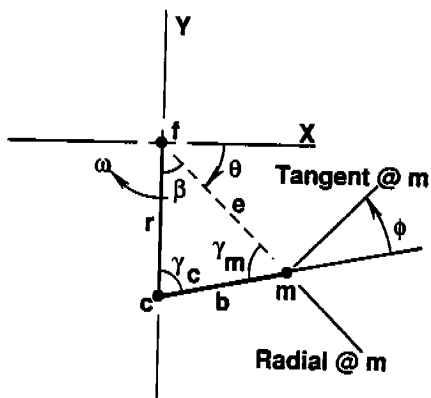


Figure 3 Kinematic model of eccentric bushing mechanism

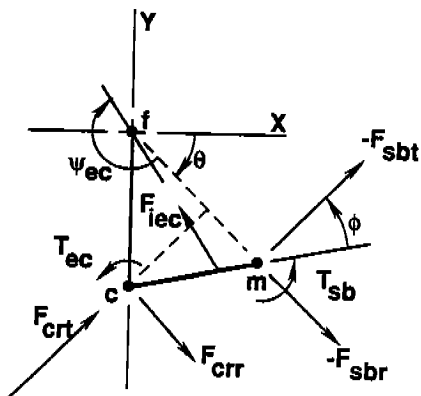


Figure 7 Free body diagram of eccentric bushing mechanism

kinematic model for this mechanism is shown in Fig. 5 where  $e$  is still the eccentricity of orbit, but  $b$  is now the offset of the slider block centerline,  $\gamma$  is the offset angle, and  $\theta$  is the crank angle. Also labeled in Fig. 5 are the tangent and radial lines to the orbiting scroll at  $m$ . The performance of the slider block radial compliance mechanism will be shown to be significantly effected by the block offset.

The geometric relationships for the eccentric bushing can be described by the following with reference to Fig. 3:

$$\cos(\beta) = \frac{e^2 + r^2 - b^2}{2 e r} \quad (1)$$

$$\cos(\gamma_c) = \frac{r^2 + b^2 - e^2}{2 r b} \quad (2)$$

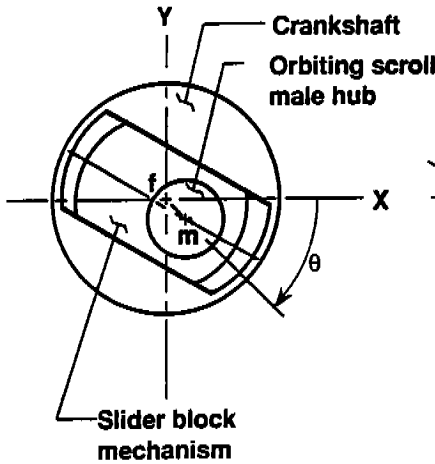


Figure 4 Slider block type radial compliance mechanism

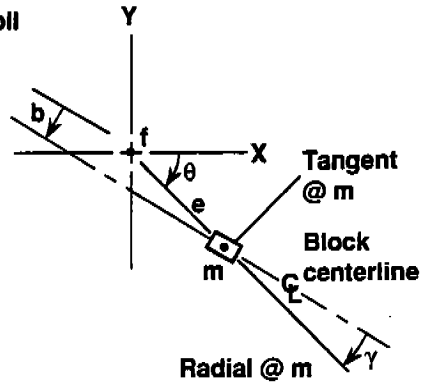


Figure 5 Kinematic model of slider block mechanism

$$\gamma_m = \pi - \beta - \gamma_c \quad (3)$$

$$\phi = \frac{\pi}{2} - \gamma_m \quad (4)$$

The geometric relationships for the slider block are simple; the offset angle is defined by the following with reference to Fig. 5:

$$\sin(\gamma) = \frac{b}{e} \quad (5)$$

### Forces

The force and moment balances on the orbiting scroll and Oldham coupling are discussed in References [1] and [3] where it is shown that simultaneous equations result and must be solved to obtain the reaction forces at the supports of the orbiter such as the bearing hub, thrust surface, Oldham keys, and scroll wrap flanks. If a fixed crank configuration is considered, it is assumed no contact occurs at the flanks of the scroll wraps and the resulting simultaneous equations from the orbiter and Oldham coupling are equal in number to the unknowns. If a radial compliance mechanism is used, there is contact at the wrap flanks and an additional unknown enters into the simultaneous equations which is the flank contact or sealing force,  $F_s$ . Now there is one more unknown than equations and an additional force or moment balance equation is required. This additional equation comes from the analysis of the radial compliance mechanism.

In Fig. 6, the primary loads on the scroll orbiter are shown [1,3] along with the reaction force at the orbiter bearing hub,  $F_{sb}$ . The forces acting on the eccentric bushing mechanism are shown in Fig. 7 and include the reaction between the orbiter hub and eccentric bushing, as well as the reactions between the eccentric bushing and crank offset, the moments due to friction at these bearing surfaces, and the inertia force of the eccentric bushing. The summation of moments about c for this mechanism yields the following equation:

$$F_{sbr} = F_{sbt} \tan(\phi) - \frac{T_{sb} + T_{ec} + F_{iec} r \sin(\psi_{ec} - \beta)}{b \cos(\phi)} \quad (6)$$

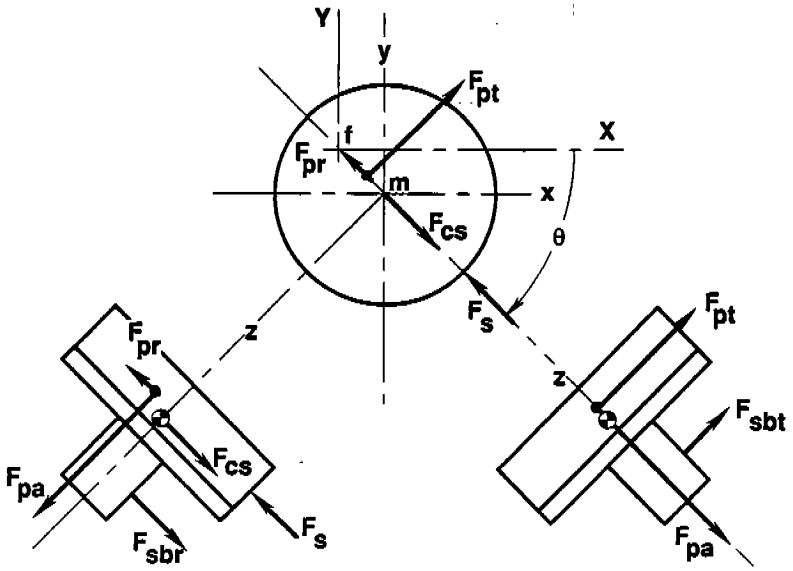


Figure 6 Forces acting on typical scroll orbiter

where

$$F_{iec} = m_{ec} e_{ec} \omega^2$$

Equation (6) is the additional equation needed to include with the simultaneous equations generated from force and moment balances on the orbiter and Oldham coupling.

The forces acting on the slider block mechanism are shown in the free body diagram of Fig. 8 and include the reactions between the orbiter hub and block, the reaction between the slider block and crank, the moment due to friction at the orbiter bearing hub, and the inertia force of the slider block. The summation of

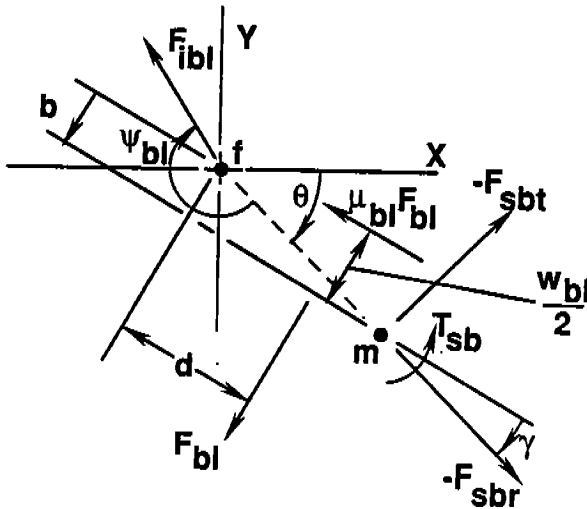


Figure 8 Free body diagram of slider block mechanism

forces and moments for this mechanism yield the following equations:

$$F_{bl} = \frac{-F_{sbt} - F_{ibl} \sin(\psi_{bl})}{\mu_{bl} \sin(\gamma) + \cos(\gamma)} \quad (7)$$

$$d = \frac{T_{sb} - F_{sbt}e}{F_{bl}} + \mu_{bl} \left[ \frac{v_{bl}}{2} - b \right] \quad (8)$$

$$F_{sbr} = F_{sbt} C_{bl} + F_{ibl} \left[ \cos(\psi_{bl}) + C_{bl} \sin(\psi_{bl}) \right] \quad (9)$$

$$C_{bl} = \frac{\mu_{bl} \cos(\gamma) - \sin(\gamma)}{\mu_{bl} \sin(\gamma) + \cos(\gamma)} \quad (10)$$

where  $F_{ibl} = m_{bl} e_{bl} \omega$

In this case, Eq. (9) is the equation needed to combine with the simultaneous equations to make the number of equations equal the number of unknowns and allow the reactions to be solved for the scroll orbiter, Oldham coupling, and slider block.

#### Actuation

The ability of these mechanisms to actuate and maintain the sealing contact between the wrap flanks of the orbiter and fixed scroll can be evaluated by deriving the radial acceleration of the orbiter for that instant in time when the wrap flanks are not in contact (due, for example, to wrap profile imperfections). In deriving the equations of motion for either mechanism, it is assumed that all linkages are rigid, and position vectors are used to define the motion of each component.

The dynamics of the eccentric bushing mechanism can be described by first defining the position vectors of points c and m as follows (referring to Fig. 3):

$$\underline{r}_c = r [ \cos(\theta+\beta) \underline{i} - \sin(\theta+\beta) \underline{j} ] \quad (11)$$

$$\underline{r}_m = \underline{r}_c + b [ -\cos(\theta+\beta+\gamma_c) \underline{i} + \sin(\theta+\beta+\gamma_c) \underline{j} ] \quad (12)$$

where  $\underline{i}$  and  $\underline{j}$  represent unit vectors in the x and y directions, respectively.

These are differentiated twice with respect to time to get the accelerations, and then the following assumptions are made: (i) steady-state compressor operation so that  $\omega$  can be considered constant, and (ii) consider the instant at which the wraps separate and lose contact so that  $\beta$  and  $\gamma_c$  can be considered constant since at the instant contact is lost no motion has yet occurred and just the angular acceleration  $\ddot{\gamma}_c$  is present. With these assumptions, the following equations result for the actuating acceleration of the orbiter when using an eccentric bushing:

$$\underline{a}_m = -r\omega^2 [ \cos(\theta+\beta) \underline{i} - \sin(\theta+\beta) \underline{j} ] + b\omega^2 [ \cos(\theta+\beta+\gamma_c) \underline{i} - \sin(\theta+\beta+\gamma_c) \underline{j} ] + b\ddot{\gamma}_c [ \sin(\theta+\beta+\gamma_c) \underline{i} + \cos(\theta+\beta+\gamma_c) \underline{j} ] \quad (13)$$

Equation (13) represents the acceleration of the orbiter, in terms of x and y components, at the instant the wraps lose contact with the mating fixed scroll. In terms of radial and tangential components, this becomes:

$$a_{mr} = \ddot{\gamma}_c b \sin(\beta + \gamma_c) - \omega^2 e \quad (14)$$

$$a_{mt} = \ddot{\gamma}_c b \cos(\beta + \gamma_c) \quad (15)$$

From these equations it is clear that besides the centripetal acceleration component  $\omega^2 e$  in the radial direction, there is a radial and tangential component due to the angular acceleration  $\ddot{\gamma}_c$  of the eccentric bushing about the c axis. This angular acceleration is an unknown value which must be determined in order to evaluate how well the eccentric bushing mechanism will operate. Thus, this angular acceleration must be incorporated into the equations of equilibrium for the scroll orbiter and eccentric bushing. Equations (14) and (15) are incorporated into the previous simultaneous force and moment equations using d'Alemberts principle by retaining the previous centrifugal inertia forces and adding the inertia forces due to the unknown angular acceleration of the eccentric bushing  $\ddot{\gamma}_c$  as well as setting  $F_s = 0$  since there is now no reaction support for the orbiter at the wrap flanks. In making these additions, Eq. (6) becomes

$$F_{sbr} = F_{sbt} \tan(\phi) - \ddot{\gamma}_c C_{ec1} + C_{ec2} \quad (16)$$

$$C_{ec1} = \frac{m_{ec} e_{ec} \left( e_{ec} - e \cos(\psi_{ec} - \beta) \right)}{b \cos(\phi)} \quad (17)$$

$$C_{ec2} = - \frac{T_{sb} + T_{ec} + F_{iec} r \sin(\psi_{ec} - \beta)}{b \cos(\phi)} \quad (18)$$

The same procedure is followed to obtain the acceleration of the orbiter with the slider block mechanism. Referring back to Fig. 5, the following equations result for the slider block if the same steps are taken as described above for the eccentric bushing.

$$\underline{r}_m = b [ \cos(\theta + \beta) \underline{i} - \sin(\theta + \beta) \underline{j} ] + c [ \sin(\theta + \beta) \underline{i} + \cos(\theta + \beta) \underline{j} ] \quad (19)$$

$$a_{mr} = \ddot{c} \sin(\beta) - \omega^2 e \quad (20)$$

$$a_{mt} = \ddot{c} \cos(\beta) \quad (21)$$

As with the eccentric bushing, the accelerations just defined for the slider block, Eqs. (20) and (21), are incorporated into the previous simultaneous force and moment equations using d'Alemberts principle. From these changes Eq. (9) now becomes

$$F_{sbr} = F_{sbt} C_{b1} + \ddot{c} C_{b12} + C_{b13} \quad (22)$$

$$C_{b12} = m_{b1} ( C_{b1} \cos \beta - \sin \beta ) \quad (23)$$

$$C_{b13} = F_{ib1} ( \cos \psi_{b1} + C_{b1} \sin \psi_{b1} ) \quad (24)$$



### DYNAMIC CHARACTERISTICS

The above described equations were used to analyze the forces and actuating acceleration in a prototype scroll compressor for both the eccentric bushing and slider block mechanisms. Starting with the eccentric bushing, the tangent angle  $\phi$  is varied with the crank offset kept constant in Figs. 9 and 10. The total average sealing force between the wraps is plotted in Fig. 9, along with the average radial acceleration which will actuate the orbiting scroll to move radially outward. In Fig. 10, the total average sealing force is plotted with the average bearing loads reacted by the scroll bearing hub and upper crankshaft bearing. It is clear from Fig. 9 that maximum values for sealing force and radial actuating acceleration exist for the eccentric bushing. The maximum of each do not coincide, however the maximum radial acceleration does occur at a tangent angle which has a reasonably large sealing force. In Fig. 10 it is clear that some sensitivity of the bearing loads to  $\phi$  occurs with the maximum values coinciding with the maximum sealing force.

The crank offset  $r$  is varied in Figs. 11 and 12 as a ratio referenced to a base value. The variables plotted in Figs. 11 and 12 are the same as in Figs. 9 and 10 and show that as the crank offset is increased, the sealing force, actuating acceleration, and bearing loads also increase.

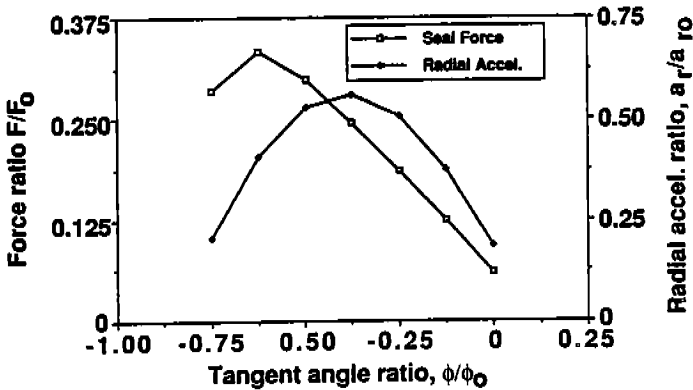


Figure 9 Effect of tangent angle on seal force and actuating acceleration

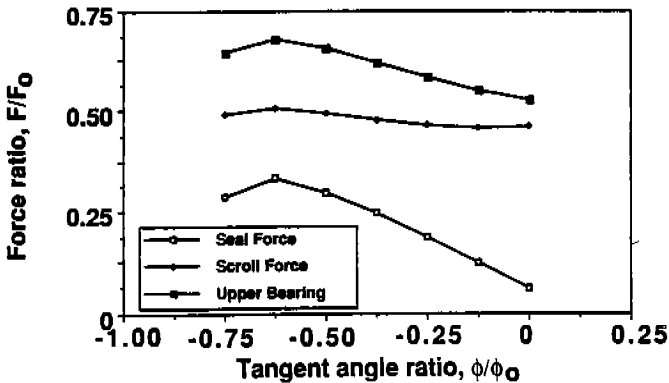


Figure 10 Effect of tangent angle on seal force and bearing reactions

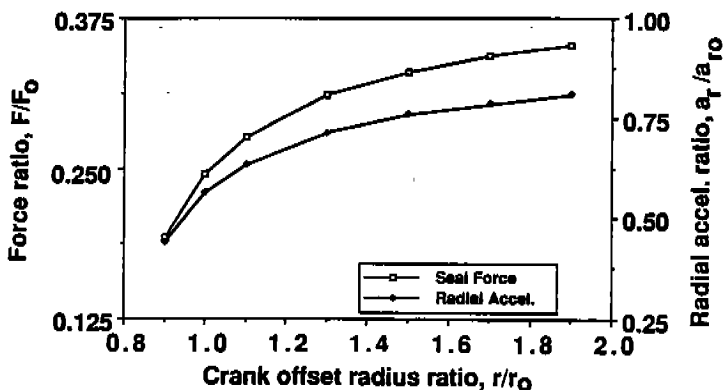


Figure 11 Effect of crank offset on seal force and actuating acceleration

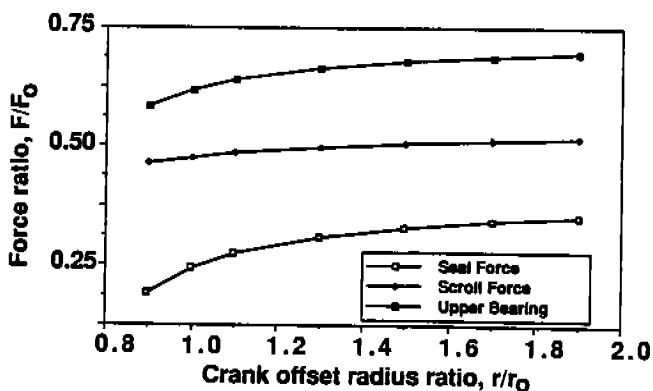


Figure 12 Effect of crank offset on seal force and bearing reactions

In Figs. 13 and 14, results for the slider block mechanism are shown in which the offset angle is varied. In Fig. 13, the total average sealing force between the wraps is plotted along with the average radial acceleration which will actuate the orbiting scroll to move radially outward. In Fig. 14, the total average sealing force is plotted along with the average bearing loads reacted by the scroll hub, the slider block/crank interface, and by the upper crankshaft bearing. Again, the radial acceleration which will actuate the orbiter is calculated for the condition when the orbiting scroll wraps have instantaneously separated from the mating fixed scroll wraps such that no radial motion of the orbiter has yet taken place. From Fig. 13, it is again clear that a maximum value exists for the radial acceleration of the orbiter. As with the tangent angle for the eccentric bushing, an offset angle exists for the slider block where the radial acceleration is maximum and at which there is a large sealing force. Also, as was seen in Fig. 10 for the eccentric bushing, the bearing loads in Fig. 14 increase as the sealing force increases. It should be noted that the maximum acceleration in Fig. 13 is much higher than the maximum in Fig. 9 for the eccentric bushing, and similarly the sealing force at the maximum acceleration is much higher for the slider block than for the eccentric bushing.

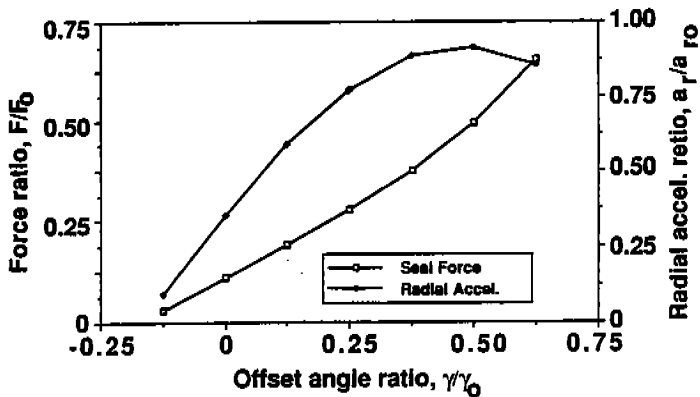


Figure 13 Effect of offset angle on seal force and actuating acceleration

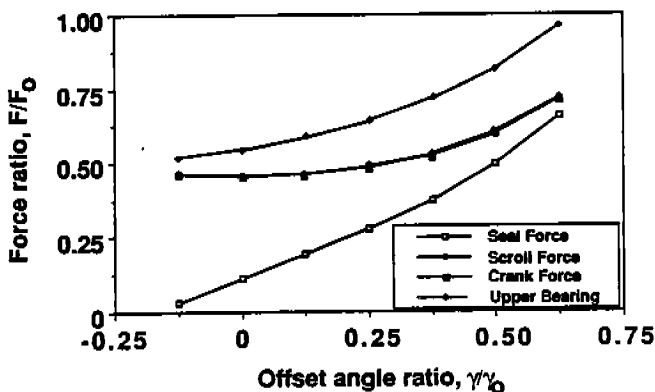


Figure 14 Effect of offset angle on seal force and bearing reactions

### CONCLUSIONS

Two major conclusions can be drawn from these results:

- (1) The operation, in terms of reaction forces and actuating acceleration, of an eccentric bushing or slider block radial compliance mechanism is very sensitive to geometry. Consequently, the analytical tool described herein is quite useful for determining the most effective radial compliance mechanism.
- (2) Within reasonable space limitations, the slider block mechanism can be designed to provide greater sealing force and actuating acceleration than the eccentric bushing.

### REFERENCES

1. Morishita, E., et al., "SCROLL COMPRESSOR ANALYTICAL MODEL", Proc. of the 1984 Intern. Compr. Eng. Conf. (Purdue), July 1984, pp. 487-495.
2. Inaba, T., et al., "A SCROLL COMPRESSOR WITH SEALING MEANS AND LOW PRESSURE SIDE SHELL", Proc. of the 1986 Intern. Compr. Engr. Conf. (Purdue), Aug. 1986, pp. 887-900.
3. Hirano, T., et al., "DEVELOPMENT OF HIGH EFFICIENCY SCROLL COMPRESSORS FOR AIR CONDITIONERS", Proc. of the 1988 Intern. Compr. Engr. Conf. (Purdue), July 1988, pp. 65-74.